THERMOMECHANICAL BEHAVIOUR AND PRESSURE SENSING OF CERAMIC WIRELESS DEVICES FOR HIGH-TEMPERATURE ENVIRONMENTS

Peter Sturesson[1, 2,3], Zahra Khaji[2], Stefan Knaust[2], Lena Klintberg[2], and Greger Thornell[1, 2]

[1]Ångström Space Technology Centre, Department of Engineering Sciences, Uppsala University, Uppsala, Sweden
[2]Division of Microsystems Technology, Department of Engineering Sciences, Uppsala University, Uppsala, Sweden
[3]Division of Military Technology, Department of Military Sciences, Swedish National Defence College, Stockholm

E-mail: peter.sturesson@angstrom.uu.se

Abstract
This paper reports on the design, fabrication and thermomechanical characterization of wireless ceramic devices, one with an integrated pressure sensor element. The project aims at developing microsystems for sensing in harsh environments where conventional electronic devices are restrained. Here, the devices are LC resonating circuits made from High-Temperature Co-fired Ceramic (HTCC) aluminium oxide green tapes. For the fabrication, the tapes were screen-printed with platinum paste, micromachined, stacked, laminated and fired. The additional sensor element was made from the same material and with the same processes, and contains a cavity sealed with a capacitive membrane. Thermomechanical characterization was made by investigating the bimorphic behaviour due to CTE mismatch as well as the resonance frequency of the devices as a function of mechanical displacement. Also, the resonance frequency as a function of pressure was demonstrated for the device with an integrated pressure sensor node. The wireless readings were performed with a tuneable resonating loop antenna. The devices showed a relatively low quality factor value. The bimorphic behaviour is low with only small variations for temperatures up to 400°C. As for the mechanical displacement, the resonance frequency was only affected for thin devices at forced deformations that were larger than those observed as a function of temperature. For the device with an integrated pressure sensor, a clear pressure-induced frequency shift of 6785 ppm was observed at 1.5 bar. This indicates that the devices are robust for high temperatures and also applicable for pressure readings. Future work will further expand on high-temperature characterization of the devices.

Introduction
Sensing in harsh environments implies a number of specific requirements, such as high temperature, high pressure, corrosion and erosion. For conventional electronic circuits, temperature requirements usually span between -55 and 125°C, a temperature range also denoted military standard [1]. However, for space, as well as for military aviation, temperature and pressure can exceed this by far. Vehicles must be able to sustain surface temperatures up to 450°C and pressures up to 90 bar in order to survive [2]. In jet and rocket engines, monitoring combustion-related parameter, such as gas pressure, gas-flow velocity and temperature are critical in order to optimize the performance [3]. In a modern jet engine for fast jet systems, temperature and pressure span between 20 and 1450°C and 1 to 26 bar respectively [4]. At temperatures above 600°C, silicon, which is a common material for microsensors, is not mechanically reliable [5], wherefore alternative materials are needed. At the same time, mismatch in thermal expansion as well as wired connections are causing challenges in inter-facing.

Ceramic devices can be fabricated with Low-Temperature Co-fired Ceramic (LTCC) or High-Temperature Co-fired Ceramic (HTCC) technology, and thus have the potential to sustain temperatures up to at least 600°C and 1000°C, respectively [6]. Fonseca, Radosavljevi and Xiong et al. have demonstrated LTCC-based double membrane pressure sensors for temperatures up to 550°C [7-

9]. It has, however, not been studied how integrable these devices are into larger systems. As thermally induced changes in different materials can, in addition to interfacing and wiring challenges, influence the performance, these changes need to be investigated.

This paper presents the design, fabrication and initial thermomechanical characterization of a wireless device. Further on, the device is also demonstrated with an integrated pressure sensor node.

Design, materials and fabrication

The antenna is an LC resonance circuit consisting of a multi-turn planar square loop and a 3.6×3.6 mm capacitor parallel-plate capacitor centred in the loop, figure 1 (left). The coil conductor width is 250 µm, and the isolation distance is 250 µm.

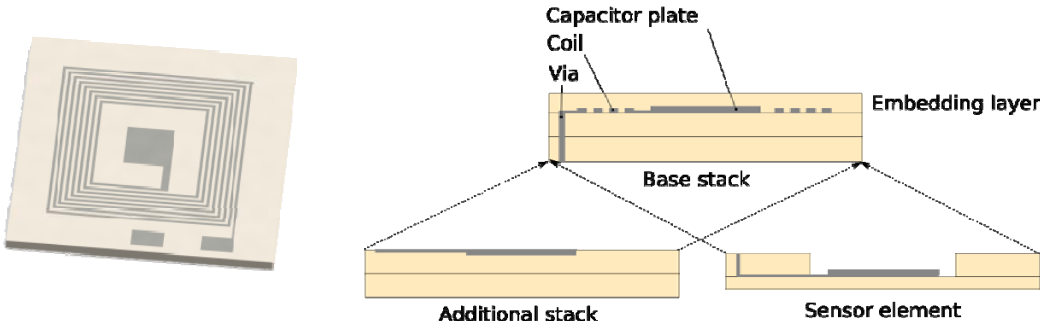

Figure 1. *Tilted top-view of the top-layer of the device (left), and a cross-section schematic divided into: base stack, the additional stack and the pressure sensor element (right).*

The resonance frequency of the circuit is described by:

$$f = {}^{1}\!\!\diagup\!\!_{2\pi\sqrt{LC}}, \tag{1}$$

where L is the inductance of the planar loop and C is the capacitance, which can be described as:

$$C = \varepsilon_0 \varepsilon_r \frac{A}{d}, \tag{2}$$

where ε_0 is the permittivity in vacuum, ε_r is the dielectric constant, A is the capacitor plate area, and d is the capacitor plate distance. The geometric dependence of the resonance frequency implicates that geometrical changes due to thermal expansion may influence the resonance frequency of the circuit. Also, temperature dependent changes in the dielectric constant can be expected to have influence.

The devices were fabricated from ceramic green tapes consisting of 99.96% alumina (ESL 44007-150/130/50 µm, Electro Science Laboratories, USA) as bulk. Platinum pastes (ESL 5542/5571, ESL Electro Science Laboratories, USA) were used for electrical conductors and the capacitor.

The conducting patterns of the LC circuit were screen-printed on separate 150 µm thick green tapes through a 325 lines per inch mesh and dried for 15 minutes at 50°C. After aligning the green tape sheets, a via with 150 µm radius was milled using a PCB plotter (Protomat S100, LPKF, Germany) and filled with platinum paste. The top layer, consisting of one of the capacitor plates and the planar coil, was embedded with a 50 µm thick sheet, acting as a base stack. To vary the total thicknesses of the stack, an additional stack, comprising of 4 or 5 150 µm thick sheets, was added as the bottom layer of the LC circuit, figure 1 (right).

For the pressure sensor device, a 130 µm thick layer with a milled circular cavity of 6 mm radius was added below the top layer. The bottom layer was screen-printed on a 50 µm thick sheet, and placed over the cavity. For mechanical support, a graphite fugitive insert (ESL 49000, Electro Sciences Laboratories, USA) was milled out and placed in the cavity.

As a reference to the wireless samples, one sample was fabricated without embedding and stacking layers, allowing it to be connected with wires.

The green tape stacks were laminated at 21 MPa and 70°C for 20 minutes in a hydraulic laminator (RMP 210, Bungard, Germany). After lamination, the samples were contoured to 23×21 mm single devices. In the final fabrication step, the samples were fired in a high-temperature furnace (ECF 20/18, Entech, Sweden) following a temperature profile suited for removing organic binders in the green tape and all of the fugitive insert, and for sintering the alumina and platinum. The initial ramping paces were 60°C/hour to a dwell temperature of 140°C, to 170°C and 200°C at 10°C/hour, to 375°C at 14°C/hour and 550°C at 40°C/hour in order to allow the organic binder to decompose and disappear. For the pressure sensor device, an additional ramping pace of 60°C/hour between 550 and 800°C was added in order to decompose and remove the fugitive insert. Finally, the temperature was increased to 1550°C at 300°C/hour where the samples were sintered for two hours.

The resulting samples with resonance frequencies and thicknesses are listed in table 1.

Table 1. *Device IDs, total thicknesses, and resonance frequencies.*

Device number	Frequency [MHz]	Thickness [µm]
1	45	410
2	44	760
3	46	890
4 (w pressure sensor)	58	530
5 (wired)	49	410

Characterization

The quality factor was evaluated from the input port voltage reflection coefficient, S_{11}, using a vector network analyser, VNA, (Fieldfox 9923, Agilent, USA).

Thermally induced deflections of Devices 1- 3 were measured for different device thicknesses at temperatures up to 400°C in an in-house fabricated laser profilometer. In this, a Kanthal–wired hotplate was mounted on a translation stage, possible to position in two directions, and a laser measurement system (OD5, SICK, Germany) was mounted above it to measure the distance to the device while the platform was displaced in one direction with 0.5 mm steps. The radius of curvature was extracted from the discrete distances with a curve-fitting algorithm.

The resonance frequency dependency on mechanical deformation was measured on Devices 1-3 and 5 during three-point bending (AGS-X, Shimadzu, USA) with the load increasing from 0-10 N in steps of 0.5 N. Devices 1-3 were wirelessly powered and read using a loop antenna with a main loop made from a 4-mm diameter copper tube with a matching loop, milled out from a PCB. For tuning the loop antenna to the devices, a trimmer capacitor was soldered to the main loop. The loop antenna was placed around the device under test. Device 5 was powered and read through wire. All devices were connected to the VNA logging the shift of the S_{11} parameter.

For the pressure induced resonance frequency shift, Device 4 was placed inside a polymer pressure chamber being pressurized from normal atmospheric pressure up to 2.5 bars in steps of 0.3 bar. Here, a different loop antenna, with the trimmer capacitor substituted with a varactor diode (BB201.215, NXP, The Netherlands), controlled by an external voltage supplier, was employed. The capacitance was shifted in steps of 1.1 pF at the rate of 1.6 Hz, allowing the resonance frequency of the loop antenna to be swept over the response signal of the device while the S_{11}-signal was logged with an ENA series network analyzer (E5072A, Agilent, USA). By plotting the minimum magnitude of the S_{11}-samplings, the response from the devices could be characterized with the maximum of the minimas corresponding to the resonance frequency, figure 2.

In order to confirm the sustainability of the devices, they were heated to 1000°C, and Device 4 was in addition pressurized to 4.5 bar while being heated to 1000°C. Here, an in-house furnace with a Kanthal heater coil clamped between two aluminium nitride plates was used. The temperature was monitored with a Type K thermocouple.

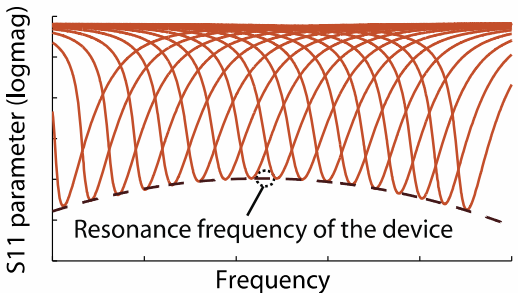

Figure 2. *Frequency sweep of the loop antenna when placed 5 cm above a device. The resonance frequency of the latter is found at the maximum of the fitted line.*

Results

The lamination and firing of the samples show a resulted in a monolithic structure and adequate embedment of the conducting pattern, figures 3 and 4.

All devices maintained their performance after the temperature and pressure testing.

The devices exhibited a quality factor value of 6.7 in average with a standard deviation of 0.61.

The thermally induced, normalized radius of curvature, figure 5, changed between 0.99 and 1.04 for Device 1, between 0.85 and 1.07 for Device 2, and between 0.98 and 1 for Device 3. In the wirelessly monitored bending tests, figure 6, Devices 1 and 2 showed no resolvable shift until reaching a normalized radius of curvature of 0.4 and 0.6 respectively. The maximum relative frequency shifts were -80 and -180 ppm, respectively. For Device 3, the shift could not be resolved. For the wired Device 5, a similar pattern was observed, albeit with a higher order of magnitude, with almost no frequency shift until a change of the normalized radius of curvature of about 0.5, figure 7. A maximum frequency shift of 56600 ppm was reached at the minimum normalized radius of curvature.

The pressure-induced relative frequency shift shows a nearly linear shift with a slightly lower shift between 1.2 and 1.5 bar, figure 8. The total relative frequency shift was 6785 ppm at 1.5 bar. It was also confirmed that the resonance frequency returned to the original value when the pressure was decreased to atmospheric pressure.

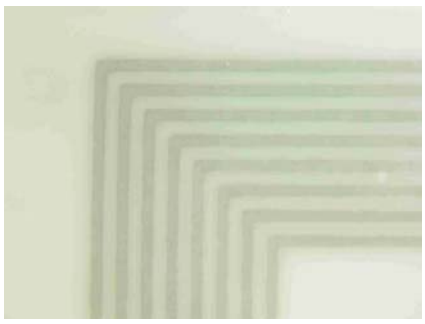

Figure 3. *Stereo microscope close-up image of the planar loop through the embedding layer.*

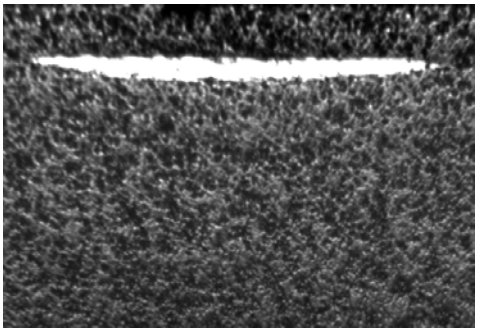

Figure 4. *Light microscope cross-section view of one turn (bright) of the planar loop with the embedding layer on top.*

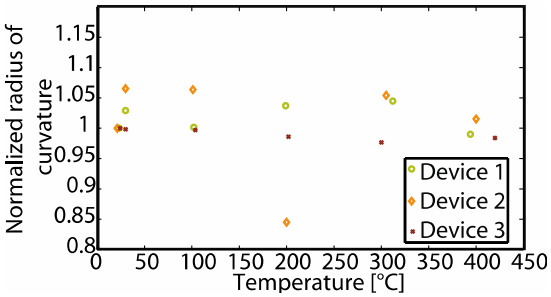

Figure 5. *Normalized radius of curvature versus temperature.*

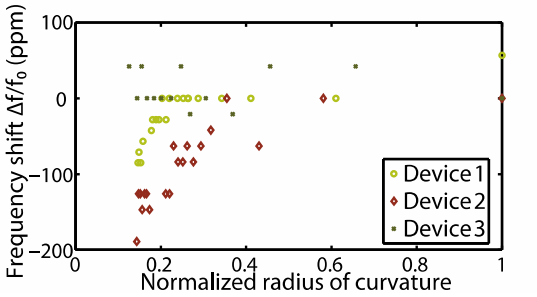

Figure 6. *Relative frequency shift versus normalized radius of curvature versus temperature from wireless reading.*

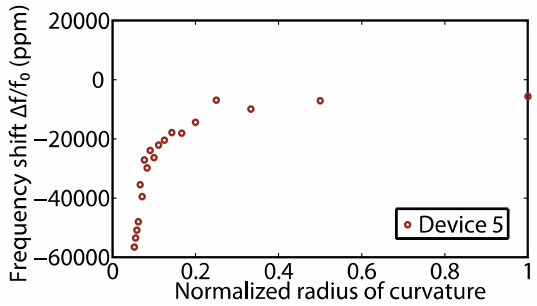

Figure 7. *Relative frequency shift versus normalized radius of curvature versus temperature from wired reading.*

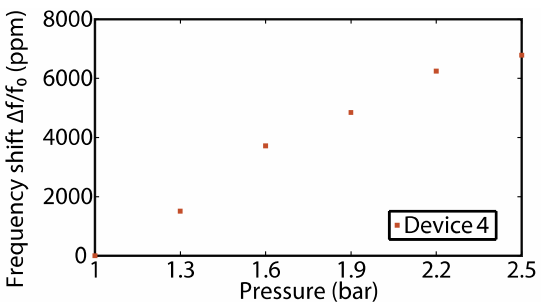

Figure 8. *Relative frequency shift versus pressure from atmospheric pressure to 2.5 bars.*

Discussion and conclusions

The obtained quality factor value is considered to be low, which is believed to be related to the intrinsic low quality factor value of planar loops, to the low thickness of the screen-printed conductors, and to the relatively low conductance of the platinum paste. Changes in the thermally induced bimorphic behaviour of the samples are low. Variations of the normalized radius of curvature related to device thickness do not follow a clear trend but indicates that the variations are less for thick samples than for thin ones. However, it can be concluded that the devices are thermomechanically robust.

Changes in the wirelessly read relative resonance frequency during three-point bending are very small, and resolvable shifts are observed at normalized radiuses of curvature that are far less than those that are observed as a function of temperature. For the wired Device 5, it is obvious that the device shifts with a larger order of magnitude than what is wirelessly measured. It does, however, follow a similar pattern indicating that the devices can be deformed significantly without the resonance frequency being severely affected.

For the pressure sensor device, a clear pressure-induced signal can be extracted and observed. The small change between 1.2 and 1.5 bar indicates that the membrane has reached the bottom of the cavity.

Altogether, these results are very promising for the continuation of the work, which will focus on pressure characterization at high temperatures up to 1000°C.

Acknowledgements

The Knut and Alice Wallenberg foundation is acknowledged for funding the laboratory facilities. The Centre for Natural Disasters Science (CNDS, a part of the Governmental Strategic Initiative) is acknowledged for part of the funding. Andreas Tenggren at Agilent Technologies Sweden AB and Anders Lund at the Department of Chemistry at Uppsala University are acknowledged for contributing with hardware and knowledge. Klas Hjort is acknowledged for his good advice.

References

[1] US DoD 2008, *Test Method Standard,* MIL-STD-810G

[2] Landis GA 2006 Acta Astronaut **59** 570-579

[3] Spang III H A and Brown H 1999 *Control of jet engines* **7** 1043-1059

[4] GKN Aerospace

[5] Domnich V, Aratyn Y, Waltrand M K, and Gogotsi Y 2008 *Rev. Adv. Mat. Sci.* **17** 33-41

[6] Lekholm V, Persson A, Palmer K, Ericson F, and Thornell G 2013,*J. Micromech. Microeng.* **23**

[7] Fonseca M A, English J M, von Arx M, and Allen M G 2002 *J. Microelectromechanical Systems,* **11** 337-343

[8] Radosavljevic G J, Zivanov L D, Smetana W, Maric A M, Unger M, and Nad L F 2009 *IEEE Sensors Journal* **9** 1956-1962

[9] Tan Q, Kang H, Xiong J, Qin L, Zhang W, Li C, Ding L, Zhang X, and Yang M 2013 *Sensors* 13 9896-9908